doi:10.1017/S1431927621006188
Microsc. Microanal. 27 (Suppl 1), 2021

Cryo-EM structure of the flight muscle thick filament from the bumble bee, *Bombus ignitius*, at 6 Å Resolution

Jiawei Li[1], Hamidreza Rahmani[2], Fatemeh Abbasi Yeganeh[2], Hosna Rastegarpouyani[1], Dianne Taylor[2], Hiroyuki Iwamoto[3] and Kenneth Taylor[4]

[1]Institute of Molecular Biophysics, Florida State University, Tallahassee, Florida, United States, [2]florida state university, United States, [3]Japan Synchrotron Radiation Research Institute, United States, [4]Florida State University, Florida, United States

Striated muscles from vertebrates and invertebrates are thought to have evolved separately from a common bilaterian ancestor [1]. Despite widely different morphological features, the muscle structure and the contraction mechanism in striated muscle are surprisingly conserved. Thick filaments in striated muscle are much more diverse when compared to thin filament but are also much less understood. Molecular structures of thick filaments could contribute toward resolving the phylogenetic relationships among different species. Asynchronous flight muscles, which empower higher wingbeat frequency with less energy consumption, are found in only four insect orders - Hemiptera, Diptera, Hymenoptera and Coleoptera. All are thought to have evolved independently from the same ancestor [2]. Hemiptera, which appeared around 373 Mya are the oldest order [2]. Thick filament structures have been obtained from the fruit fly *Drosophila melanogaster* [3], a Dipteran, and the giant waterbug *Lethocerus indicus* [4], a Hemipteran. Here we describe a structure from the bumble bee, *Bombus ignitius*, a Hymenopteran.

Dorsal longitudinal muscles were dissected from thoraces preserved at -80° in 80% glycerol. After washing out the glycerol using a relaxation buffer containing ATP and EGTA, Z-disks were digested with calpain and actin filaments depolymerized using calcium insensitive gelsolin. *Bombus* thick filaments with sufficient concentration to obtain multiple filaments in each hole of a 2/1 copper Quantifoil grid were plunge frozen in liquid ethane and grids examined on the Titan Krios operated at 300keV. Images were recorded on a K3 camera operated in counting mode. Each micrograph consisted of 75 frames. After motion correction and CTF estimation, around 120,000 overlapping segments (particles) were manually picked and extracted into 768 x 768 pixel boxes in Relion [5] (Fig. 1a). The 2D classification and 3D auto-refinement are processed by cisTEM [6], around 110,000 particles were selected after 20 rounds of 2D classification. We used a previously determined *Lethocerus indicus* thick filament reconstruction [4] low pass filtered to 60 Å resolution as reference and imposed only C4 symmetry during reconstruction. After 37 rounds of 3D refinement, a 3D structure was obtained at ~5Å resolution as quantified by FSC (Fig. 1b). Overall resolution including the myosin heads is 6 Å. Map sharpening was necessary to compensate the contrast lost in high resolution. Local resolution was also estimated by Local Monores [7] and the map was proportionally sharpened according to the spatially varied resolution values by Local Deblur [8] as implemented in Scipion [9]. As a result, the backbone of the filament was sharpened better than the heads, proximal S2 region and the paramyosin core. The overall resolution was slightly dampened. The quality of the sharpening is biased by the mask threshold. The sharpening mask was generated by Relion. The 768 x 768-pixel box contains less than half the length of the myosin molecule's tail. Utilizing the filament's helical symmetry, determined and imposed using Relion, the 5-crown reconstruction was extended to 12-crowns which facilitated segmentation of a single myosin tail and its arrangement into myosin ribbons (Fig. 1c). The map was displayed and segmented by Chimera [10].

The arrangement of myosin tails is consistent with the "curved molecular crystalline layers" model [11] as seen in *Lethocerus* and *Drosophila*. All three thick filaments have similar helical parameters as reported by Relion using relion_helix_toolbox. The axial repeat of *Bombus*, *Drosophila* and *Lethocerus* thick filaments is

145 Å as measured by X-ray fiber diffraction [12]. Measurements by cryoEM were larger at 147.533 Å for *Bombus*, but similar to the value obtained for the other thick filaments [3,4]. The helical twist angle of *Bombus* is 34.05°, which is higher than 33.86° and 33.92° of *Drosophila* [3] and 33.98° of *Lethocerus* [4]; the minor difference may not be statistically significant. Unlike *Lethocerus* [4] but like *Drosophila* [3], the myosin heads in *Bombus* are disordered (Fig. 1d). Unlike *Drosophila* there appears to be no protein binding the backbone outer surface that might explain the disorder. Among the coiled-coil tail a noticeable difference is a Skip 1 region slightly less-angled with respect to the surface in *Bombus* (Fig. 1d) compared to the *Lethocerus*. Other unique *Bombus* features are exhibited among non-myosin proteins. *Bombus* myofilin, a non-myosin protein found within the filament backbone of both *Lethocerus* and *Drosophila*, presents some novel densities not seen in either (Fig 1e); the flightin molecules are similar among all three species. All apparently extend a disordered domain outside of the filament backbone which evidence suggests is the N-terminus [13]. *Lethocerus* shows the largest amount of this extension, which contacts its proximal S2 [4]. More of the flightin extension is seen in *Bombus* than Drosophila (Fig. 1b,e). The central core of the *Bombus* filaments as seen in raw images and averaged projections of the reconstruction is dense like that of *Lethocerus* and unlike the hollow core seen for *Drosophila* (Fig. 1a). *Bombus* paramyosin, like that of *Lethocerus*, is highly visible in the filament central core (Fig. 1f), but differs from *Drosophila* where no paramyosin was visible. Many features of the *Bombus* thick filament are similar to *Lethocerus*, the older of the four orders. Other features are shared with Drosophila, but *Bombus* has a number of features in common with neither. We are pursuing protein sequence analysis as one method to interpret the non-myosin elements of the structure, and obtain more information from the mass spectroscopy is also in our future research plan. Supported by NIGMS/NIH.

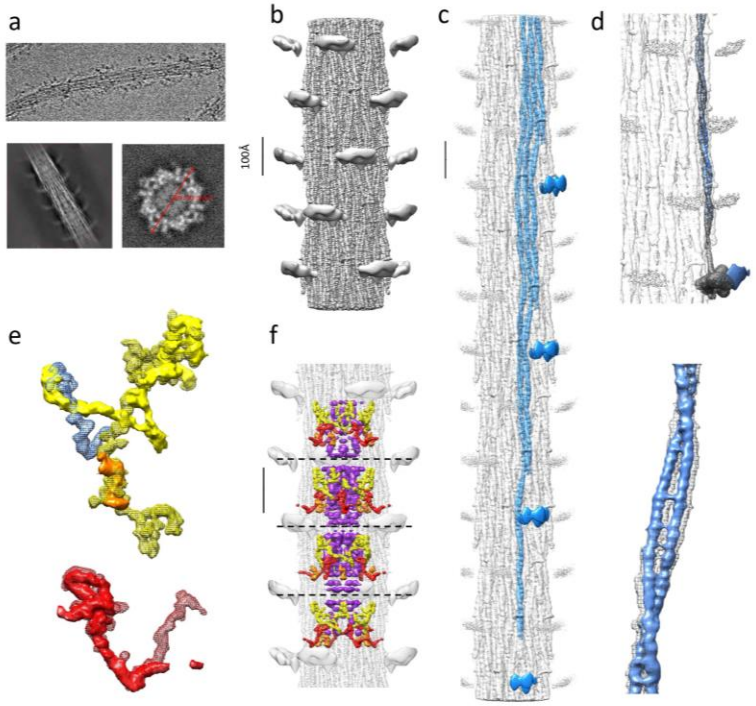

https://doi.org/10.1017/S1431927621006188 Published online by Cambridge University Press

Figure 1. (a) Top: electron micrograph of the *Bombus* thick filament with good contrast. Bottom: one of the 2D class images in 768*768 pixel box (left) and the cross-section view of the 3D model (right) showing the dense core of the *Bombus* thick filament. (b) The reconstructed 5-crown *Bombus* thick filament at ~6Å, the flightin tails extend out of the thick filament surface (circled by red rings). (c) The 12-crowns pseudofilament produced by extending using helical symmetry, one ribbon is highlighted. (The myosin heads are blurred in the extended map because the different contour threshold is used to show the whole ribbon) (d) Top: the *Bombus* myosin head (blue) is disordered as shown in different density compared to the *Lethocerus* (grey). Bottom: the alignment of Skip 1 region between *Bombus* (blue) and *Lethocerus* (grey) showing the slightly different orientation with respect to the backbone surface. (e) The comparison of the non-myosin densities between *Lethocerus* (meshed) and *Bombus* (solid). Top: The *Bombus* myofilin has two densities (colored in yellow and orange), that overlap and contact both the myofilin and "blue" protein described in the *Lethocerus* structure; Bottom: *Bombus* and *Lethocerus* flightin highly superimpose except for the extended tail. (f) *Bombus* paramyosin (purple) and nonmyosin proteins shown in context.

References

1. Steinmetz, Patrick R. H., Johanna E. M. Kraus, et al. *Nature* 487, no. 7406 (July 2012): 231–34.
2.
2. Misof, B., S. Liu, et al. *Science* 346, no. 6210 (November 7, 2014): 763–67.
3. Daneshparvar, Nadia, Dianne W Taylor, et al. *Life Science Alliance* 3, no. 8 (August 2020): e202000823.
4. Hu, Zhongjun, Dianne W. Taylor, et al. *Science Advances* 2, no. 9 (September 2016): e1600058.
5. Zivanov, Jasenko, Takanori Nakane, et al. *ELife* 7 (November 9, 2018): e42166.
6. Grant, Timothy, Alexis Rohou, and Nikolaus Grigorieff. *ELife* 7 (March 7, 2018): e35383.
7. Vilas, Jose Luis, Josué Gómez-Blanco, et al. *Structure* 26, no. 2 (February 2018): 337-344.e4.
8. Ramírez-Aportela, Erney, Jose Luis Vilas, et al. Edited by Lenore Cowen. *Bioinformatics*, August 26, 2019, btz671.
9. Rosa-Trevín, J.M. de la, A. Quintana, et al. *Journal of Structural Biology* 195, no. 1 (July 2016): 93–99.
10. Pettersen, Eric F., Thomas D. Goddard, et al. *Journal of Computational Chemistry* 25, no. 13 (October 2004): 1605–12.
11. Squire, J.M. *Journal of Molecular Biology* 77, no. 2 (June 1973): 291–323.
12. Squire, John M., Tanya Bekyarova, et al. *Journal of Molecular Biology* 361, no. 5 (September 2006): 823–38.
13. Gasek, Nathan, Lori Nyland, and Jim Vigoreaux. *Biology* 5, no. 2 (April 27, 2016): 16.